Laboratory Evidence for Surface Nucleation of Solid Polar Stratospheric Cloud Particles

A. Tabazadeh,*,† Y. S. Djikaev,‖ P. Hamill,§ and H. Reiss‖

NASA Ames Research Center, Moffett Field, California 94035, Department of Physics, San Jose State University, San Jose, California 95192 and Department of Chemistry and Biochemistry, UCLA, Los Angeles, California 90095

Received: April 24, 2002; In Final Form: August 13, 2002

Nitric acid-containing cloud particles, known as polar stratospheric clouds, play an important role in the springtime ozone destruction over the polar regions. Nitric acid initially condenses in the polar stratosphere to form supercooled solution droplets of mainly nitric acid and water with trace amounts of sulfuric acid. Nitric acid dihydrate (NAD) and nitric acid trihydrate (NAT) later crystallize from this supercooled solution phase to form solid polar stratospheric cloud particles. Until now, experimental data on this crystallization process has been analyzed under the assumption that NAD and NAT nucleation took place in the interior volume of a cloud droplet. However, in this paper, reanalysis of experimental data on the homogeneous freezing rates of concentrated aqueous nitric acid solution droplets provides substantial support for the occurrence of nucleation "pseudoheterogeneously" at the air−aqueous nitric acid solution interface of the droplet. Furthermore, in a following paper, theory that provides compelling evidence for such interfacial nucleation is developed. Together, the reanalysis of laboratory data in this paper and the supporting theoretical arguments in the following paper suggest that the homogeneous nucleation process occurring in atmospheric droplets may be a surface- rather than a volume-related rate process.

1. Introduction

It was first suggested in 1986 that some polar stratospheric cloud (PSC) particles may contain nitric acid[1,2] because they were observed in the stratosphere at temperatures above the ice frost point.[3] In situ aerosol composition measurements later confirmed that PSC particles do contain nitric acid.[4−6] Nitric acid trihydrate (NAT) was suggested to be the likely phase of nitric acid particles in the stratosphere.[1] Later, laboratory observations showed that NAT is stable in the stratosphere at temperatures of approximately 5 K above the ice frost point.[7] Other laboratory experiments indicated that nitric acid dihydatre (NAD) can also form in the stratosphere.[8,9] In addition, Worsnop et al.[9] found that the metastable NAD phase readily formed in the laboratory, whereas the stable NAT phase was only formed by conversion of NAD into NAT.

In situ observations from the Airborne Arctic Stratospheric Expedition (AASE) further complicated the understanding of nitric acid particle formation by providing evidence for the presence of liquid-phase sulfate particles at cold polar temperatures.[10] Prior to the AASE observations, solid nitric acid particles were assumed to nucleate on the surfaces of frozen sulfuric acid tetrahydrate (SAT) particles (the most stable $H_2SO_4-H_2O$ phase under polar stratospheric conditions).[11] Soon after the AASE observations were published, laboratory investigations showed that aqueous sulfuric acid can remain liquid, and absorb a substantial amount of HNO_3 at cold polar temperatures.[12,13] Laboratory data[13] were later used in aerosol models[14,15] to show that nearly all HNO_3, available in the atmosphere, could potentially condense into the $H_2SO_4-H_2O$ liquid solution to form a liquid ternary aerosol (LTA) consisting of $H_2SO_4-HNO_3-H_2O$. The fact that both solid[1,8,9] and liquid states[13−15] were suggested for nitric acid-containing cloud particles in the stratosphere was in agreement with lidar observations of PSCs, which indicated the frequent occurrence of both particle types in the stratosphere.[16−18]

LTA particles in the stratosphere form by condensational growth such that a nucleation free energy barrier does not have to be overcome,[14,15] and currently, there is no debate on how LTA particles form and grow in the stratosphere. In contrast, even after more than a decade of research on PSCs, a quantitative understanding on the formation mechanism of solid nitric acid-containing cloud particles is still lacking.[19] Previously, it was thought that the most likely mechanism involved the heterogeneous nucleation of nitric acid hydrates on the surfaces of ice particles.[19] However, ample evidence from observational data seems to indicate that solid nitric acid clouds in the stratosphere often form independent of ice clouds.[18,20−22] To account for the formation of solid nitric acid particles in the stratosphere (above the ice frost point) several suggestions have been made involving homogeneous[23,24] and heterogeneous[22,25] freezing of the LTA system. In this paper, we reexamine laboratory data on homogeneous freezing of NAD and NAT to show that this process most likely initiates on the surface of a supercooled cloud droplet rather than within its bulk volume.

2. Background on Surface Nucleation

Common examples of nucleation in fluids, such as bubble formation[26] and the crystallization of drops of molten metal,[27] involve liquid−vapor or liquid−liquid interfaces. However, as far as we know, until now, laboratory studies and theoretical models[22−24,28−37] of the freezing of atmospheric particles have

* To whom correspondence should be addressed. E-mail: atabazadeh@mail.arc.nasa.gov.
† NASA Ames Research Center, Moffett Field.
§ Department of Physics, San Jose State University.
‖ Department of Chemistry and Biochemistry, UCLA.

10.1021/jp021045k CCC: $22.00
Published on Web 10/02/2002

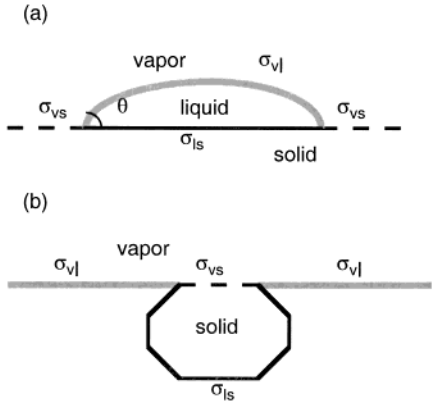

Figure 1. (a) Partially wetting drop of liquid (lens shaped) resting on a solid substrate surrounded by vapor. The three interfaces are vapor−liquid (vl, gray line), vapor−solid (vs, dashed line), and liquid−solid (ls, black solid line). The corresponding surface tensions are σ_{vl}, σ_{vs}, σ_{ls}. θ is the contact angle. (b) Crystal nucleus in a liquid, but with one face in contact with the vapor. Black solid line indicates faces in contact with the liquid while the face in contact with the vapor is represented by the dashed line.

assumed that freezing occurs via nucleation within the particle volume. A recent analysis of laboratory data[35−37] on the freezing of supercooled water droplets suggests that this process may also be a result of ice nucleation at the droplet surface (air−water interface) rather than within the droplet volume.[38] In the present paper, we reanalyze existing laboratory data[23,28−32] on the freezing rates of concentrated aqueous nitric acid solution droplets. The results of this analysis strongly suggests that this freezing process may also initiate at the droplet surface.

The idea of surface freezing is supported by several kinds of independent evidence, which even suggest that droplet surface nucleation may be the preferred mode in many atmospheric processes. For example:

1. Computer simulations show that, in fluid clusters, crystalline nuclei tend to form at or near surface layers.[39]

2. Cahn[40] has shown that, away from its critical point, a liquid is not likely to fully "wet" a solid. This could include, as a special case, a melt and its own solid.

The relevance of item 2 above is the following. Consider Figure 1a that applies to a single component system. The Figure shows a lens-shaped drop of melt (liquid) resting at equilibrium on the surface of its crystalline solid. Both solid and melt are exposed to the vapor of the same substance. The surface or interfacial tensions σ_{vs}, σ_{vl}, and σ_{ls} refer to the vapor-solid, vapor−liquid, and liquid−solid interfaces shown as dashed, gray, and solid lines, respectively. The equilibrium configuration in Figure 1a shows that the melt only partially wets its solid, and the contact angle θ exceeds zero (complete wetting would have $\theta = 0$). Such an equilibrium configuration indicates that $\sigma_{vl} + \sigma_{ls} > \sigma_{vs}$, the condition for partial wetting, and suggests that the extension of the liquid−solid interface at the expense of the vapor-solid interface would be discouraged by an increase in the total surface free energy of the overall system.

Now consider Figure 1b, which shows a schematic crystal nucleus forming within the liquid melt with one face, say of area "a", at the interface with the vapor so that it constitutes a vapor−solid interface denoted by a dashed line. If the nucleus formed entirely within the bulk of the liquid, instead of with one face in contact with the vapor, then the difference in free energy would reflect that the free energy $\sigma_{vs}a$ would be replaced by $\sigma_{ls}a + \sigma_{vl}a$ (assuming that the new face was also of area a) corresponding to the two new interfaces, vapor−liquid and liquid−solid, that replace the single interface, vapor-solid. The difference in free energy would therefore be $\sigma_{ls}a + \sigma_{vl}a - \sigma_{vs}a$. If the nucleus formation at the surface was favored, then this free energy difference would be positive such that $\sigma_{ls} + \sigma_{vl} - \sigma_{vs} > 0$, which is identical with the condition for partial wetting presented above. Thus, crystallization at the vapor−liquid interface should be favored in cases where the solid is only partially wettable by its own liquid melt.

The above argument is only qualitative, but in the following paper,[41] we derive a more rigorous thermodynamic criterion to show how the determination of the contact angle between a solid an its melt can be used to predict the mode (surface or volume) of nucleation. This criterion indeed proves to be the condition of partial wetting suggested qualitatively above.

To test whether the partial wetting criteria can be used to determine the mode of nucleation in the atmosphere, we briefly discuss the ice−water system. Optical studies on surface melting of ice show that water only partially wets the ice surface.[42] This observation suggests that ice nucleation in supercooled water most likely occurs on the droplet surface. In fact, our recent analysis[38] of ice nucleation kinetic data,[35] where water droplets studied were immersed in various ambient oil baths, show that the ice-nucleation line (nucleation rate versus temperature) yields a different slope in different oils. This observation suggests that ice nucleation most likely have occurred on water droplet surfaces because the only physical property that changes when the oil is changed is the water−oil interface and not the bulk properties of pure water. In other words, if ice nucleation had occurred in the bulk of water droplets, then the rates of ice nucleation should not have varied in different ambient oil baths. Thus, at least for the ice−water system the condition of partial wetting leading to surface nucleation of ice in water seems to hold.

The case of nitric acid hydrate crystal nucleation in aqueous nitric acid solution droplets involves a multicomponent (at least a binary) system, and the simple vapor of the preceding discussion is replaced by air with its several components. Thus, to make the argument more convincing, it will be necessary to derive a criterion (or criteria) for surface versus volume nucleation in *multicomponent* systems. The thermodynamics will be complicated, not only by the presence of several components, but also by the need to consider surface adsorption by all components. Nevertheless, in a future paper, we plan to derive such extended criteria.

In the remainder of the present paper, we reexamine existing laboratory data on the nucleation of NAD and NAT crystals in highly concentrated aqueous nitric acid solution droplets. The manner of analysis indicates that this nucleation process is most likely surface rather than volume based.

3. Relation between the Interpretations of Experimental Data as Volume or Surface Nucleation

Homogeneous freezing of a supercooled liquid droplet in the atmosphere can occur when a crystal nucleus forms either within the volume of the droplet or on its surface. Although a single nucleus is sufficient to crystallize a supercooled liquid droplet, the nucleation rate is often expressed as J_V the number of nuclei formed per second in a unit volume of the liquid. Similarly, let J_S be the number of nuclei formed per second on unit surface area of the liquid. Thus, the total number of crystal nuclei formed per unit volume of air per second is

$$J_T = J_V V_t + J_S S_t \quad (1)$$

where V_t and S_t are the total volume and surface area of all

droplets per unit volume of air. In atmospheric studies of homogeneous freezing to form either ice or nitric acid hydrate particles (both NAT and NAD) from aqueous solutions, it is always assumed that $J_T = J_V V_t$.[22−24,28−37] This assumption ignores the potential effect of nucleus formation at the surface of a liquid aerosol particle.[27,38,39,41] In fact, if the free energy of liquid formation is lower on the surface of a particle than within its bulk,[41] then the overall rate of particle freezing will be proportional to the total available aerosol surface area and not to aerosol volume.

In atmospheric sciences, a standard expression for the rate of homogeneous crystal nucleation within the bulk of a fluid (J_V) is given by[43]

$$J_V = N_L(kT/h)\mathrm{EXP}\left[\frac{-\Delta G^b_{act}}{RT}\right] \quad (2)$$

This represents a crude approximation based on the original theory of absolute reaction rates (there are better expressions today), but it is good enough for our analysis, given the accuracy of the experimental data. In eq 2, N_L is the molecular solute concentration in the liquid (for our case N_L is the molecular concentration of HNO_3 in the liquid solution per cm^3 of volume), k and h are the Boltzmann and Planck constants, T is the temperature in Kelvin, R is the gas constant, and ΔG^b_{act} is the free energy of formation, in the bulk, of the crystal nucleus. A similar relation for J_S the rate of nucleus formation on the droplet surface is

$$J_S = N_S(kT/h)\mathrm{EXP}\left[\frac{-\Delta G^s_{act}}{RT}\right] \quad (3)$$

where N_S is the total number of molecules per unit surface area of the fluid (for our case $N_S = X_{HNO_3} n_S$, where X_{HNO_3} is the mole fraction of HNO_3 on the surface of the liquid solution and $n_S = 10^{15}$ is the approximate number of molecular surface sites per cm^2 of surface area of the liquid[43]), and ΔG^s_{act} is the free energy of formation of a crystal nucleus on the droplet surface.

If we assume that homogeneous freezing occurs in the laboratory, solely due to nucleus formation on particle surfaces, then the reported volume-based freezing rates[23,28−32] are related to surface-based rates by the following expression

$$J_S = (V_t/S_t)J_V \quad (4)$$

Note that in deriving the above relation, we have assumed that formation of just one nucleus is sufficient to freeze a single droplet in the ensemble of those monitored in the laboratory.[23,28−32] Thus, the measured number of droplets that freeze in unit time can be expressed as either $J_V V_t$ or $J_S S_t$, depending upon which mechanism (volume or surface based) is assumed. If the distribution of droplet sizes is monodisperse, then eq 4 reduces to

$$J_S = (r/3)J_V \quad (5)$$

where r is the aerosol droplet radius. Thus, if the nucleation process is surface-based, different rates of freezing would be observed, depending on the droplet size distribution. For example, a larger fraction of droplets will freeze if the aerosol volume is spread over many small droplets[28,30−32] than if it were confined to a few larger ones.[23] Below, eqs 4 and 5 are used to convert reported volume-based rates into surface-based rates for NAT and NAD particle formation from droplets of concentrated aqueous HNO_3. These rates are then used in eq 3 to derive ΔG^s_{act} values for NAT and NAD formation in the stratosphere.

TABLE 1: Laboratory Freezing Investigations

type	sample size	experimental technique[a]	references
film	1−2 μm	FTIR	Tisdale et al.
aerosol	∼0.5 μm particles	cloud chamber/FTIR	Disselkamp et al. Anthony et al. Prenni et al.
aerosol	∼0.38 μm particles	flow-tube/FTIR	Bertram and Sloan
aerosol	∼25 μm particles	optical microscopy/ visual inspection	Salcedo et al.

[a] In the aerosol experiments (except for Anthony et al. where LTA solutions were used) binary aqueous nitric acid solutions were used. Aqueous nitric acid solutions were also used in the film experiments.

4. Interpretation and Analysis of Laboratory Nucleation Rates

Table 1 lists the laboratory investigations discussed below. First, data from aerosol experiments[23,28,30−32] are used to derive surface-based nucleation rates for NAT and NAD formation. Second, results from film experiments[45] are used to provide support for the idea that the nucleation of NAD crystals from aqueous nitric acid solutions occurs at the surface layer of a droplet.

Figure 2 shows laboratory reported aerosol nucleation freezing rates over a temperature range from 165 K to 205 K for different solution compositions (the HNO_3 mole fraction, X, is given on the bottom of each panel). All of the Figure 2 panels (except for panel (d) where NAT nucleation freezing rates are shown) show laboratory freezing rates for NAD aerosols. Equations 4 and 5 were used to convert the reported volume rates (filled symbols) into surface rates (open symbols).

In Figure 2a, nucleation data for nitric acid solutions with concentration $X_{HNO_3} = 0.333$ are shown from three laboratories.[23,28,30−32] At temperatures above 190 K, the volume based data (filled symbols) exhibit considerable discrepancy, especially between triangles[23] and the other symbols.[28,30] This discrepancy in laboratory data is as great as 4 orders of magnitude. Furthermore, nucleation rates should decrease with increasing temperature, but some of the data, due to Disselkamp et al.,[28] admittedly limited, suggests either an increase or no change in the rate as temperature is increased. Yet there is no obvious experimental reason for the discrepancy (Margaret Tolbert, personal communication, 2001). In contrast to this behavior, when eqs 4 and 5 are used to convert the rates, reported as volume based (filled symbols), to surface based (open symbols) rates, most of the discrepancy disappears as is evident from the open symbols in the lower part of Figure 2a. Not only do the data from different laboratories now lie within about only 1 order of magnitude of each other, but also now they all trend downward with increase in temperature, a functional dependence that is expected. This result provides support for a surface based nucleation mechanism.

What could be the origin of the discrepancy in the volume based data? The best answer involves eq 5, which shows that if indeed nucleation is surface based, then the size of the aerosol droplets must play a strong role. In the experiments of Salcedo et al.,[23] the average size of an aerosol droplet was 25 microns, whereas in the experiments of Prenni et al.[30] and Disselkamp et al.,[28] the droplet size was of the order of 0.5 microns. Thus, on the basis of eq 5 alone, assuming that nucleation *was* surface

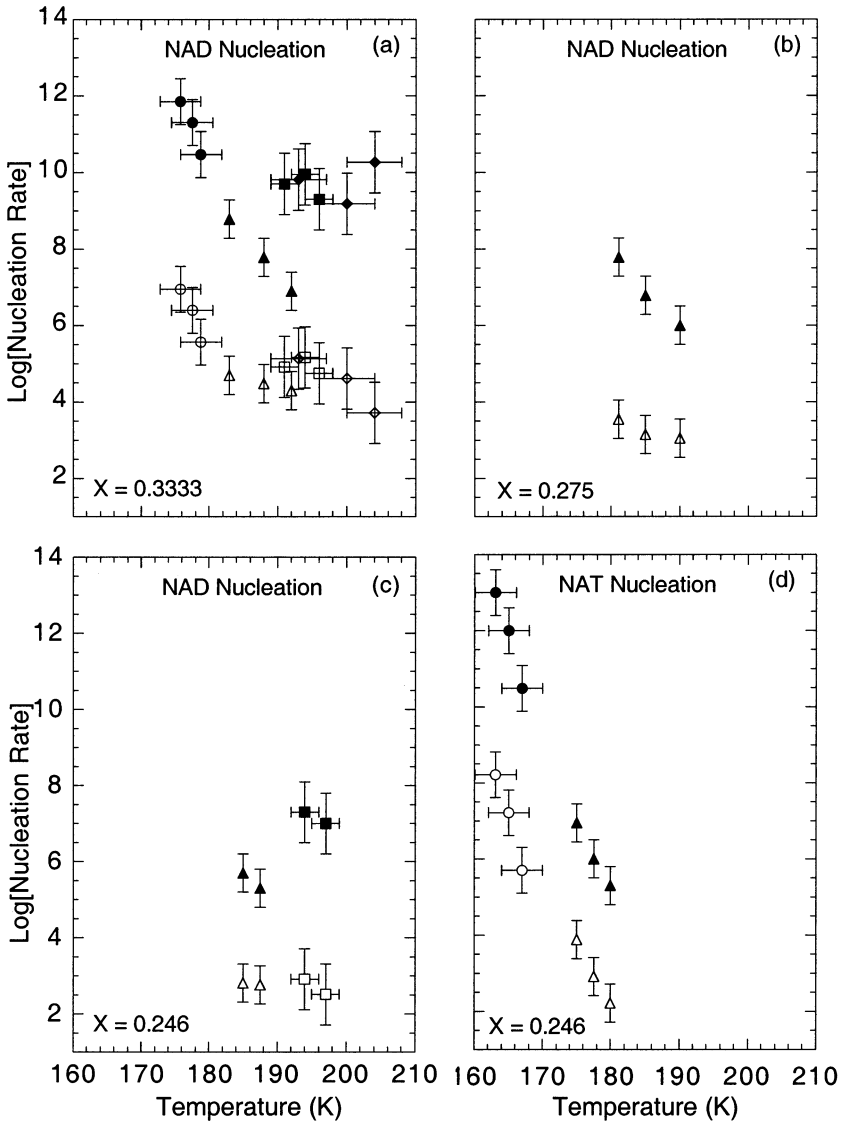

Figure 2. Volume- and surface-based nucleation rates of NAD (panels a, b and c) and NAT (panel d) aerosols from aqueous HNO_3 solutions determined by laboratory observations. Filled and open symbols give volume (in units of cm^{-3} sec^{-1}) and surface (in units of cm^{-2} sec^{-1}) rates, respectively. Circles are from Bertram and Sloan (BS),[31,32] Triangles are from Salcedo et al. (SA),[23] squares are from Prenni et al. (PR),[30] and diamonds are from Disselkamp et al. (DI).[28] The HNO_3 mole fraction of the solution (X) is given on the bottom of each panel. The surface rates are derived from the reported volume-based nucleation rates using eqs 4 and 5. For BS data a monodisperse size distribution with a mode radii of 0.38 micron was used. For PR data, a monodisperse size distribution with a mode radii of 0.5 micron was used. For DI the size distributions given in Table 1 of this article were used. For SA, the large supermicron-sized particles (~25 micron in radius) immersed in oil were nonspherical and therefore the measured geometric aspects of particles were used to convert volume to surface area. For SA, the average behavior of many data points are shown only as few symbols. This was done to give equal weight to data reported from all laboratories for the determination of the nucleus free energy of formation.

based and that surface rates were similar in all cases, the Salcedo et al.[23] results should lie, as they do, far below the results of the other investigators. Actually, the aerosol of Salcedo et al.[23] (triangles) was eventually immersed and caused to freeze in a matrix of oil, so that an oil−aqueous nitric acid rather than an air−aqueous nitric acid interface was involved. Thus, we cannot really be sure that the surface rates were similar for both interfaces. Also, in the Salcedo et al.[23] case, the droplets were not entirely spherical and a more realistic geometry than that assumed in the derivation of eq 5 was used in converting the assumed volume rates to surface rates. Nevertheless, the case for surface nucleation remains compelling.

Figure 2c provides similar support, in the NAD case, for surface nucleation. It exhibits data of Salcedo et al.[23] and Prenni et al.[30] for nitric acid solutions of concentration $X_{HNO_3} = 0.246$. Again, the filled symbols indicate the assumed volume based rates, whereas the open symbols indicate the surface rates obtained by transforming the observed assumed volume rates. Once more, there is a reduction of the discrepancy from almost 3 orders of magnitude to less than 1 order of magnitude.

It is of interest to estimate the free energies of formation of the nuclei for the surface based nucleation rates. For this purpose, all of the data for the assumed surface based rates exhibited in Figure 2a−2d were used in eq 3 to estimate the ΔG^s_{act} for both NAD and NAT nucleation in aqueous nitric acid. Although, these measured rates show a considerable scatter, they are still useful in estimating free energies because of the exponential relation between rate and free energy (i.e., in taking the logarithm to extract the free energy, the scatter is considerably reduced). This is a typical feature of most nucleation

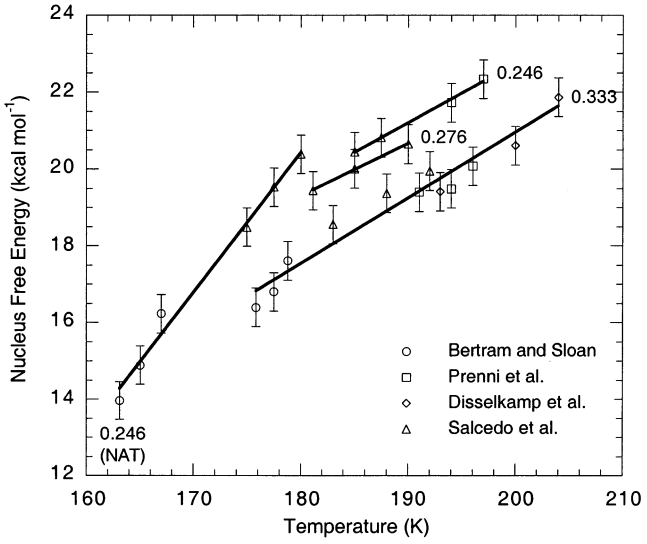

Figure 3. Surface-based nucleation rates shown in Figure 2 were used in eq 3 to derive nucleus free energy of formation for NAD (HNO_3 mole fraction = 0.246, 0.278, and 0.333) and NAT (HNO_3 mole fraction = 0.246) in aqueous HNO_3 solutions. A least-squares-fit line is shown for each solution composition and phase. The error bars (± 0.5 kcal mol^{-1}) show the range of variation in the nucleus free energy from the least-squares-fit line. The error bars do not reflect experimental uncertainty and only show deviation of points from the theory line.

phenomena. Estimates obtained in this way are plotted in Figure 3. The estimated free energies range between 40 and 55 RT (for T taken nominally as 190 K), which is typical for most nucleation processes. The lines plotted in Figure 3 can be used to establish empirical fits for the dependence of formation free energies on both temperature and nitric acid concentration. In this connection, Salcedo et al.[23] have recently used laboratory volume-reported rates in eq 2 to extract ΔG^{b}_{act} for NAT and NAD nucleus formation. In their estimates of ΔG^{b}_{act}, only the results from Salcedo et al. (triangles in Figure 2)[23] and Bertram and Sloan (circles in Figure 2)[31,32] were used in the parametrization of ΔG^{b}_{act}, mainly because (as discussed above) the volume-reported laboratory rates from Prenni et al. (squares in Figure 2)[30] and Disselkamp et al. (diamonds in Figure 2)[28] were up to 4 orders of magnitude higher than those reported by Salcedo et al.[23] Because the surface-reported rates show much less discrepancy, in our estimates, we have used all the reported laboratory nucleation data rates on the freezing of NAD and NAT aerosols. The resulting formation free energy for the NAD surface based nucleus, obtained through an empirical fitting of our estimates is given (in units of kcal mol^{-1}) by the expression

$$\Delta G^{s,NAD}_{act}(X_{HNO_3}, T) = 11.5593 + 0.080\,421\,4T - \{71.5133 - 0.256\,724T\}X_{HNO_3} \quad (6)$$

whereas that for NAT is

$$\Delta G^{s,NAT}_{act}(0.246, T) = -45.2429 + 0.364\,844T \quad (7)$$

We were not able to derive a direct composition dependence for the NAT free energy because NAT nucleation rates were available only for a single acid concentration, namely X_{HNO_3} = 0.246 (Figure 2d). However, because in Figure 3 the slope of the free energy lines for NAD are nearly parallel, a crude expression for the NAT formation free energy composition dependence can be estimated using the NAD dependence, i.e., from

$$\Delta G^{s,NAT}_{act}(X_{HNO_3}, T) = \frac{\Delta G^{s,NAD}_{act}(X_{HNO_3}, T)}{\Delta G^{s,NAD}_{act}(0.246, T)} \Delta G^{s,NAT}_{act}(0.246, T) \quad (8)$$

where it is assumed that the changes in the slope of NAT nucleus formation free energies with acid concentration are proportional to those of NAD, along the X_{HNO_3} = 0.246 composition line. Even the most extreme points shown in Figure 3 deviate from the least-squares-fits by only about ± 0.5 kcal mol^{-1} (error bars in Figure 3). As mentioned above, ΔG^{s}_{act} depends less critically on the experimental uncertainties[23,28,30−32] (aerosol composition, aerosol size-distribution, and temperature) than the actual rate. For example, changing ΔG^{s}_{act} by 0.5 kcal mol^{-1} could alter the rates by an order of magnitude (see Figure 4).

In Figure 4, the calculated volume and surface nucleation rates are shown for two solution compositions. It is apparent that volume nucleation rates for NAD (panels a and b) are much more temperature-dependent than the estimated surface based rates. For example, for X_{HNO_3} = 0.333 (panel a), volume and surface nucleation rates between 165 and 200 K vary by 6 and 2 orders of magnitude, respectively. Disselkamp et al.[28] have been able to observe freezing of concentrated aqueous HNO_3 solutions (e.g., X_{HNO_3} = 0.333) to form NAD crystals up to a temperature of about 204 K (Figure 2a). Although a surface-based rate process can readily account for these observations, a highly temperature sensitive volume-based rate process cannot explain why NAD particles were formed in the laboratory at temperatures as high as 204 K. Disselkamp et al.[28] could detect NAD freezing only if (at least) 5% of the particles froze in about 2 h. On the basis of the measured rates, a volume rate process would have caused freezing of less than 1% of the droplets into NAD in 2 h. Therefore, we conclude that such a process would have been too slow to explain NAD formation at 204 K.

Up to now, no aerosol experiments have been able to produce NAT nuclei in compositions such that $X_{HNO_3} > 0.246$. However, at temperatures below 178 K and for X_{HNO_3} = 0.246, NAT nuclei, instead of NAD nuclei,[23,31,32] do form selectively in aerosols (see Figure 4b and 4c). This observation provides additional support for surface nucleation of NAT and NAD nuclei in aqueous HNO_3. The volume-based rates indicate that NAD nuclei (Figure 4b) still retain higher nucleation rates, compared to NAT nuclei (Figure 4c) down to a temperature of about 174 K. If the nucleation process occurred in the volume, then NAT formation should not have been observed near 178 K because at this temperature NAD volume-based nucleation rates remain a factor of 5 larger than those for NAT. On the other hand, as the temperature is lowered, the surface nucleation rate for NAT first exceeds that of NAD (X_{HNO_3} = 0.246) in the neighborhood of about 178 K, indicating that below this temperature NAT nuclei can form at a higher rate than those of NAD, in accord with the observations. Because many laboratory measurements,[23] showing NAT formation, exist in the temperature range between 174 K and 178 K, it is unlikely that a volume-based freezing process could account for these observations.

Avrami analysis of the crystallization kinetics involved in the freezing of HNO_3/H_2O films (condensed on a silicon-wafer substrate) into NAD, indicates that the nucleation of NAD occurs in a 2-dimensional (2D) field.[45] Tisdale et al.[45] suggested that the 2D nature of the observed NAD freezing rates was perhaps

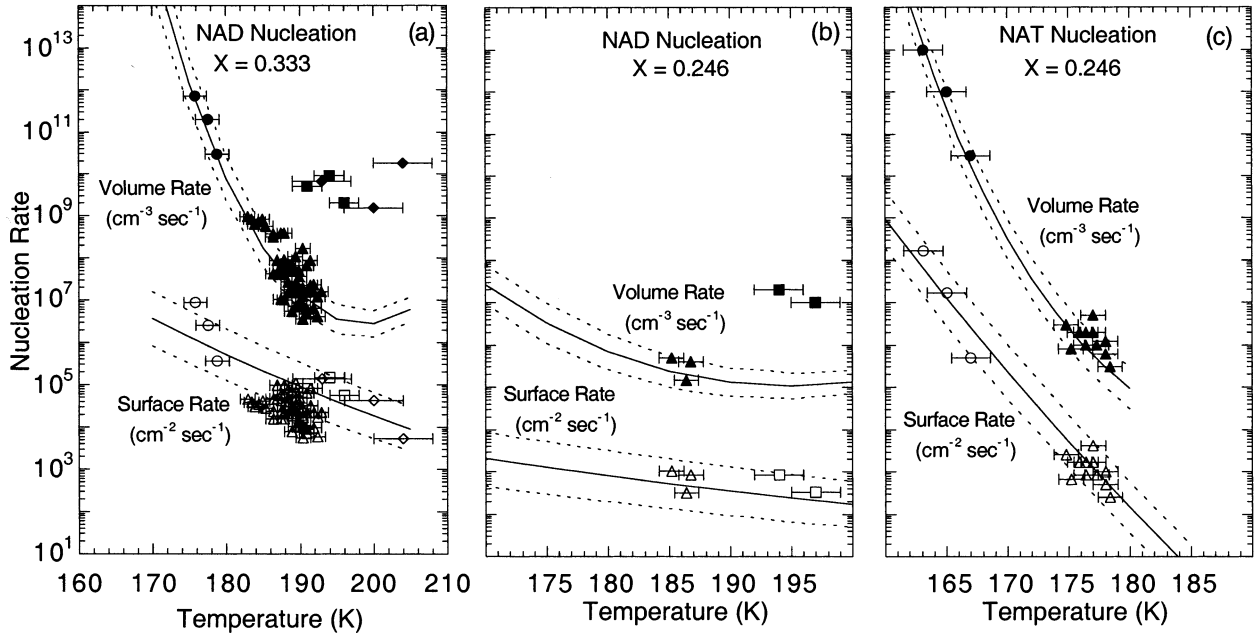

Figure 4. Calculated nucleation rates of NAD (panles a and b) and NAT (panel c) formation from 2 aqueous HNO_3 solution compositions (HNO_3 mole fraction = 0.333 and 0.246). The symbols are defined in the legend of Figure 2. All of the data points reported by Salcedo et al.[23] are shown. The volume rates are calculated using eq 2 and the nucleus free energy expressions given in Salcedo et al.[23] The surface rates are calculated using eqs 3, 6, and 7. The dotted lines give upper- and lower-bound nucleation rates obtained by using minimum and maximum possible values of nucleus formation free energies. Error bars show the reported range of temperature uncertainties.

due to heterogeneous nucleation at the film-silicon interface. However, the preceding analysis opens the alternative possibility that the observed 2D nature of the freezing rates could be the result of surface based nucleation at the aqueous nitric acid film-gas interface. With this alternative possibility, film experiments also provide some support for surface and/or 2D nucleation of NAD in aqueous HNO_3.

In arriving at the fitting formula, eq 6, for the temperature and concentration dependence of ΔG^s_{act}, we assumed that X_{HNO_3} in eq 3 is equivalent to X_{HNO_3} in the bulk of the aqueous HNO_3 droplet. This is an approximation since surface enrichment of HNO_3 should be taken into account. Indeed, recent studies in bulk aqueous HNO_3 [46] as well as in LTA[47] solutions provide evidence for the surface enrichment of HNO_3 in both systems. However, because the experiments were performed at warm temperatures, the observed enrichment might differ from that at cold temperatures. In any event, the measurements in refs 46 and 47 were not used in the development of eq 6. In the absence of significant experimental data on the surface enrichment of nitric acid at cold temperatures, it is beyond the scope of this work to attempt to quantify the level of HNO_3 enrichment in the surface layer of the LTA system.

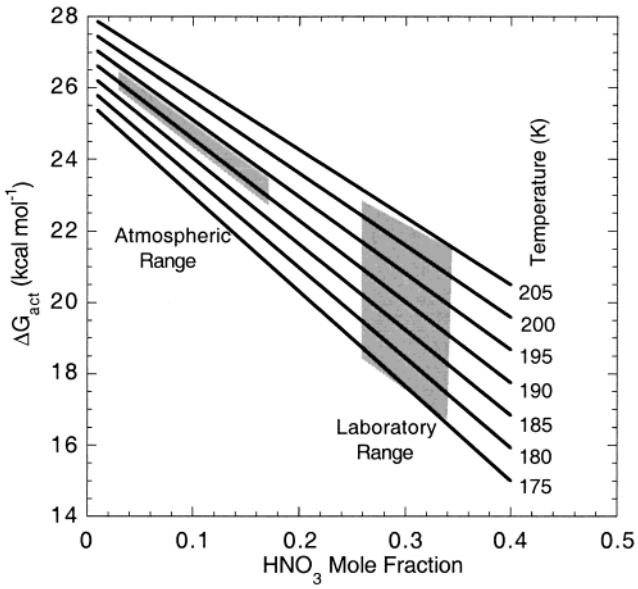

Figure 5. Calculated NAD surface nucleus free energy of formation as a function of HNO_3 mole fraction and temperature using eq 6.

5. Implications for Atmospheric Processes

The nucleation of both NAD and NAT crystals in the atmosphere takes place in LTA droplets rather than in droplets of pure aqueous nitric acid. Above, we have only derived empirical expressions for nucleation rates involving pure aqueous nitric acid. Thus, the absence of rate data for LTA droplets leaves us with the only alternative of extrapolating the current pure nitric acid results to LTA droplets. At temperatures where LTA particles freeze into hydrates of nitric acid, the H_2SO_4 acid weight percent of the LTA solution in the stratosphere drops to below about 2%.[14−15] If H_2SO_4 at cold temperatures is a surface active component, then even small amounts of sulfuric acid can cause dramatic changes in the surface tension of the solution because the nucleation free energy barrier is more sensitive to surface tension than any other parameter. However, if H_2SO_4 is not a surface active component, then we suspect that trace amounts of H_2SO_4 in LTA solutions will not significantly change the rate of hydrate formation relative to that measured in pure aqueous HNO_3. Further, even the rates derived here for pure aqueous HNO_3 are for concentrated solutions. Thus, it is not clear whether these rates will reasonably extrapolate to stratospheric compositions, where nitric acid mole fraction in droplets remains below 0.18. Because of these considerations, the discussion in the present section, in which we apply rates obtained with pure concentrated aqueous nitric acid to LTA, must be regarded as less rigorous than that in the preceding sections of this paper.

Having said this, we can turn to Figure 5 where shading indicates the composition ranges for NAD nuclei formation free energies for both the laboratory and atmospheric processes.

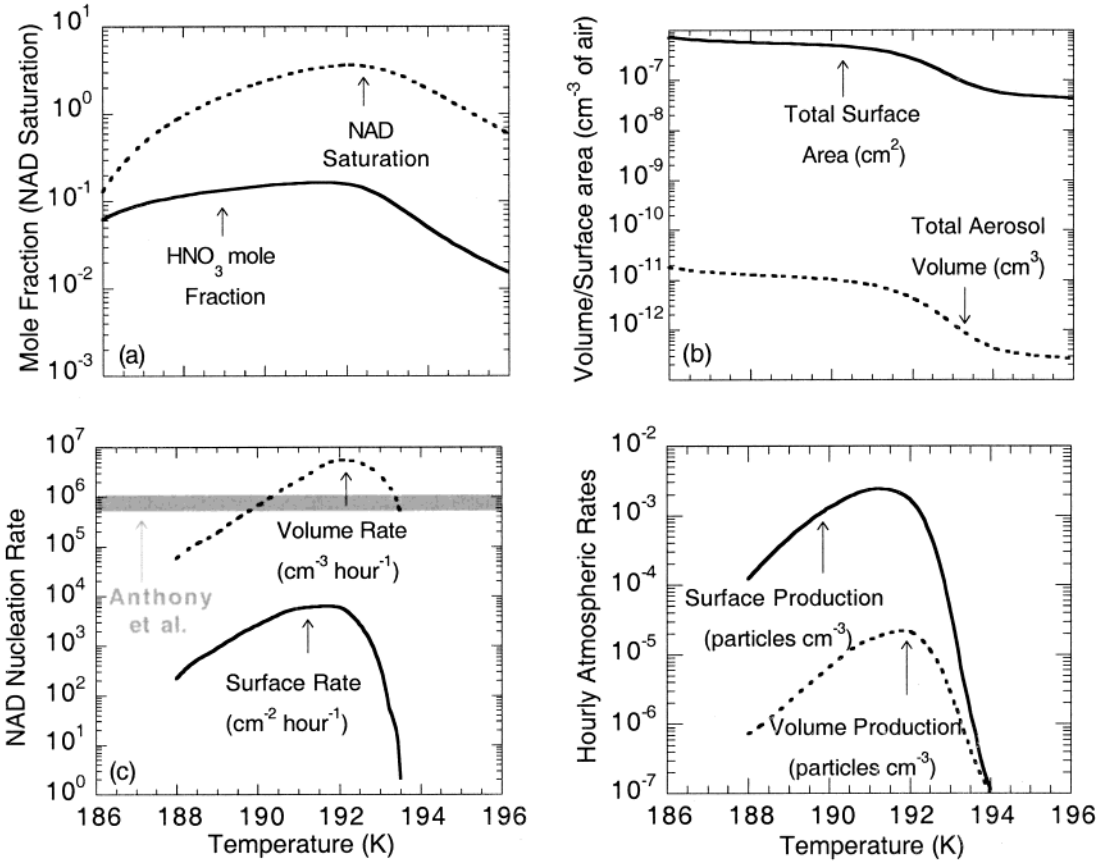

Figure 6. (a) Temperature variations in the HNO_3 mole fraction and NAD saturation. (b) Temperature variations in the total LTA aerosol surface area and volume. An assumed sulfate aerosol size distribution[10] was used to convert LTA volume into surface area (c) Temperature variations of NAD volume- and surface-based nucleation rates for LTA compositions in the stratosphere. The gray shaded area marks the possible upper-bound surface nucleation rates for LTA compositions determined in the laboratory.[29] (d) Temperature variations in the hourly stratospheric volume and surface production rates of NAD particles. All calculations were performed at 60 mb for HNO_3, H_2O and H_2SO_4 mixing ratio of 12 ppbv, 5 ppmv, and 0.5 ppbv, respectively.[48]

Clearly, these ranges are quite different. Because the laboratory compositions were more concentrated in HNO_3, NAD germ formation energies were smaller, and allowed efficient freezing to occur within minutes to at most hours, when a large ensemble of droplets ($> 10^5$ particles cm^{-3}) was studied. In the atmosphere, HNO_3 mole fraction in LTA are smaller (typically less than 0.18), and result in higher free energies of formation. Thus, in the atmosphere, longer exposure times are needed to freeze stratospheric aerosols. Also, the number densities of LTA droplets in the stratosphere are ~ 10 cm^{-3}, so that the total available surface areas in stratospheric aerosols are at least 10^4 times smaller than those available in the laboratory. This factor too will cause atmospheric aerosols to freeze more slowly than their laboratory counterparts.

Below, typical LTA aerosol nitric acid concentrations and surface areas are used to estimate (using expressions based on rates measured in pure aqueous nitric acid) the rates of nitric acid hydrate particle formation in the stratosphere. It should be emphasized and reiterated again that to obtain the results shown in Figures 5 and 6, we have extrapolated the free energy formulas derived in both the present paper, and in that due to Salcedo et al.,[23] beyond the range of the laboratory compositions.

We will deal with estimates only for NAD particle production rates in the stratosphere, because for $X_{HNO_3} \approx 0.20$ (this is the largest possible HNO_3 mole fraction in the stratospheric LTA solution), the extrapolated formation free energy for NAT is $\sim$26.2 kcal mol^{-1} (obtained from eqs 3 and 6−8). With this smallest possible value (26 kcal mol^{-1}), the hourly atmospheric NAT particle production rates are around 10^{-6} cm^{-3}. Microphysical sensitivity studies[24] have shown that hourly particle production rates below about 10^{-5} cm^{-3} cannot have a significant influence on the overall stratospheric number density of nitric acid-hydrated particles.

Figure 6, parts a and b, displays important LTA and NAD aerosol properties for solid particle nucleation in the stratosphere. To estimate volume-based nucleation rates, the NAD nucleus formation free energy due to Salcedo et al.[23] was used in eq 2. For surface-based rates, eq 3 was used. The LTA properties (NAD saturation in solution, HNO_3 LTA mole fraction, total LTA surface area and total LTA volume) are calculated using the parametrized model of Lin and Tabazadeh.[47] For a given temperature, "NAD saturation" is obtained by dividing the vapor pressure of HNO_3 over the LTA system by the equilibrium vapor pressure of HNO_3 over the NAD phase. Using the parameters shown in Figure 6a in eqs 2 and 3, we obtain the volume and surface rates shown in Figures 6c. Figure 6c gives NAD nucletion rates per unit volume and surface area of the stratospheric LTA system.

The gray band in Figure 6c marks the smallest values of surface nucleation rate that would be needed for Anthony et al.[29] to detect freezing of the LTA system in the laboratory. These authors could detect NAD freezing only if (at least) 5% of the droplets froze within about 2 h. The estimated (Figure 6c) surface based nucleation process could have caused freezing into NAD of only about 0.05% of the droplets in about 2 h. Therefore, the observations of Anthony et al.[29] on the lack of LTA freezing in the laboratory are not in disagreement with our estimates. If the volume of studied laboratory droplets could

be spread over smaller particles (to increase their surface area by a factor of roughly 100, see eq 5), then it might be possible to detect the freezing of LTA droplets in the same laboratory using experiments in the aerosol chamber (see Table 1). As discussed above, there are many advantages to formulating rate expressions using nucleation freezing rates measured in the LTA system instead of the aqueous HNO_3. For example, the presence of H_2SO_4 may increase or decrease the rate of droplet freezing in the stratosphere by affecting the level of HNO_3 enrichment at the surface layer. Thus, the direct observation of freezing rates in LTA at cold temperatures can shed light on the possible role that trace amounts of H_2SO_4 may play in the freezing process of stratospheric aerosol particles.

The products of the curves plotted in Figures 6b and 6c yields NAD particle production rates in the stratosphere (Figure 6d). For most temperatures, NAD particle production using surface-based rates is nearly 2 orders of magnitude larger than those obtained from volume-based rates. Thus, if NAD nuclei form on LTA particle surfaces, then they can nucleate at a much faster rate than nuclei that might form in the bulk solution. This finding should affect the results of microphysical calculations presented in Tabazadeh et al. work[24] because in this study extrapolated volume-based nucleation freezing rates[23] were used to calculate the rate of NAD particle production in the atmosphere. In a later publication, we intend to investigate the effect of surface nucleation in more detail.

6. Conclusions

Laboratory data on NAD and NAT nucleation rates, measured in aqueous nitric acid droplets, were used to formulate homogeneous surface-based rate expressions for the formation of solid PSC particles from LTA solutions. We showed that surface-based rate expressions for NAD and NAT particle production are consistent with all the available laboratory kinetic data on the freezing of the aqueous HNO_3 system, whereas volume-based rate expressions show considerable inconsistencies. Overall, surface-based nucleation rates of NAD particles in the stratosphere may be as many as 2 orders of magnitude larger than their corresponding volume-based rates.

The fact that NAD and NAT particle nuclei formation from an aqueous droplet seems to occur on the surface of the droplet is extremely interesting. A recent study on the kinetics of supercooled water-droplet freezing[38] suggests that this process may also occur on the surface. There is also evidence from nonatmospheric particle systems, such as crystallization of molten metal drops,[27] that the crystal nucleation occurs at an oil−liquid interfacial layer. Both computer simulations[39] and thermodynamic calculations[41] further suggest that crystalline nucleus formation is favored on the surface over that in the bulk. Thus, homogeneous (or pseudo-heterogeneous) phase transformations in atmospheric aerosols may indeed be a surface- and not a volume-related rate process. This conclusion goes against the classical theory of homogeneous crystallization, where freezing is assumed to initiate inside a droplet. In other words if the droplet crystallization process initiates at or near the surface, then atmospheric particles will freeze via propagation from the surface into the bulk instead of propagation from the bulk to the surface.

Acknowledgment. This work was mainly supported by NASA's Atmospheric Chemistry Modeling and Analysis Program and also by the National Science Foundation under Grant No. CHE-0076384. A.T. also acknowledges support from a Presidential Early Career Award for Scientists and Engineers. We thank Margaret Tolbert, Dara Salcedo and Katja Drdla for fruitful discussions.

References and Notes

(1) Toon, O. B.; Hamill, P.; Turco, R. P.; Pinto, J. *Geophys. Res. Lett*. **1986**, *13*, 1284−1287.
(2) Crutzen, P. J.; Arnold, F. *Nature* **1986**, *324*, 651−654.
(3) McCormick, P. M.; Chu, W. P.; Grams, G. W.; Hamill, P.; Herman, B. M.; McMaster, L. R.; Pepin, T. J.; Russell, P. B.; Steele, H. M.; Swissler, T. J. *Science* **1981**, *214*, 328−330.
(4) Fahey, D. W.; Kelly, K. K.; Ferry, G. V.; Poole, L. R.; Wilson, J. C.; Murphy, D. M.; Loewenstein, M.; Chan, K. R. *J. Geophys. Res.* **1989**, *94*, 11,299−11,315.
(5) Pueschel, R. F.; Snetsinger, K. G.; Hamill, P.; Goodman, J.; McCormick, M. P. *Geophys. Res. Lett.* **1990**, *17*, 429−432.
(6) Hamill, P.; Toon, O. B. *Phys. Today* **1991**, *December*, 34−45.
(7) Hanson, D. R.; Mauersberger, K. *Geophys. Res. Lett.* **1988**, *15*, 855−858.
(8) Tolbert, M. A.; Middlebrook, A M. *J. Geophys. Res*. **1990**, *95*, 22 423−22 431.
(9) Worsnop, D. R.; Fox, L. E.; Zahniser, M. S.; Wofsy, S. C. *Science* **1993**, *259*, 71−74.
(10) Dye, J. E.; Baumgardner, D.; Gandrud, B. W.; Kawa, S. R.; Kelly, K. K.; Loewenstein, M.; Ferry, G. V.; Chan, K. R.; Gary, B. L. *J. Geophys. Res*. **1992**, *30*, 8015−8034.
(11) Turco, R. P.; Toob, O. B.; Hamill, P. *J. Geophys. Res.* **1989**, *94*, 16 493−16 510.
(12) Molina, M. J.; Zhang, R.; Wooldridge, P. L.; McMahon, J. R.; Kim, J. E.; Chang, H. Y.; Beyer, K. *Science* **1993**, *261*, 1418−1423.
(13) Zhang, R.; Wooldridge, P. J.; Abbatt, J. P. D.; Molina, M. *J. Phys. Chem.* **1993**, *97*, 8541−8548.
(14) Tabazadeh, A.; Turco, R. P.; M. Z. Jacobson, M. Z. *Geophys. Res*. **1994**, *99*, 12 897−12 914.
(15) Carslaw, K.; Luo, B. P.; Clegg, S. L.; Peter, Th.; Brimblecombe, P.; Crutzen, P. *Geophys. Res. Lett.* **1994**, *21*, 2479−2482.
(16) Browell, E. V.; Butler, C. F.; Ismail, S.; Robinette, P. A.; Carter, A. F.; Higdon, N. S.; Toon, O. B.; Schoeberl, M. R.; Tuck, A. F. *Geophys. Res. Lett.* **1990**, *17*, 385−399.
(17) Toon, O. B.; Browell, E. V.; Kinne, S.; Jordan, J. *Geophys. Res. Lett.* **1990**, *17*, 393−396.
(18) Toon, O. B.; Tabazadeh, A.; Browell, E. V.; Jordan, J. *J. Geophys. Res.* **2000**, *105*, 20 589−20 615.
(19) WMO Scientific Assessment of Ozone Depletion: 1998, Rep. 44 1999.
(20) Tabazadeh, A.; Toon, O. B.; Gary, B. L.; Bacmeister, J. T.; Schoeberl, M. R. *Geophys. Res. Lett.* **1996**, *23*, 2109−2112.
(21) Tabazadeh, A.; Santee, M. L.; Danilin, M. Y.; Pumphrey, H. C.; Newman, P. A.; Hamill, P. J.; Mergenthaler, L. *Science* **2000**, *288*, 1407−1411.
(22) Drdla, K.; Schoeberl, M. R.; Browell, E. *J. Geophys. Res*., in press.
(23) Salcedo, D.; Molina, L. T.; Molina, M. J. *J. Phys. Chem.* **2001**, *105*, 1433−1439.
(24) Tabazadeh, A.; Jensen, E. J.; Toon, O. B.; Drdla K.; Schoeberl, M. R. *Science* **2001**, *291*, 2591−2594.
(25) Tolbert, M. A.; Toon, O. B. *Science* **2001**, *292*, 61−62.
(26) Talanquer, V.; Oxtoby, D. W. *J. Chem Phys*. **1995**, *102*, 2156−2164.
(27) Merry, G. A.; Reiss, H. *Acta Metall*. **1984**, *32*, 1447−1456.
(28) Disselkamp, R. S.; Anthony, S. E.; Prenni, A. J.; Onasch, T. B.; Tolbert, M. A. *J. Phys. Chem*. **1996**, *100*, 9127−9137.
(29) Anthony, A. E.; Onasch, T. B.; Tisdale, R. T.; Disselkamp, R. D.; Tolbert, M. A. *J. Geophys. Res.* **1997**, *102*, 10 777−10 784.
(30) Prenni, A. J.; Onasch, T. B.; Tisdale, R. T.; Siefert, R. L.; Tolbert, M. A. *J. Geophys. Res*. **1998**, *103*, 28 439−28 450.
(31) Bertram, A. K.; Sloan, J. J. *J. Geophys. Res.* **1998**, *103*, 3553−3561.
(32) Bertram, A. K.; Sloan, J. J. *J. Geophys. Res*. **1998**, *103*, 13 261−13 265.
(33) Tabazadeh, A.; Martin, S. T.; Lin, J. S. *Geophys. Res. Lett.* **2000**, *27*, 1111−1114.
(34) Pruppacher, H. R.; Klett., J. D. *Microphysics of Clouds and Precipitation*; D. Reidel: Dordrecht, The Netherlands, 1997.
(35) Taborek, P. *Phys. Rev. B*. **1985**, *32*, 5902−5906.
(36) Salcedo, D. *Freezing of Sulfuric and Nitric Acid Solutions: Implications for Polar Stratospheric Cloud Formation*, Ph. Thesis, Massachusetts Institute of Technology, 2000.
(37) DeMott, P. J.; Rogers, D. C. *J. Atmos. Sci*. **1990**, *47*, 1056−1064.
(38) Tabazadeh, A.; Djikaev, Y. S.; Reiss, H. *Nature*., to be submitted.
(39) (a) Chushak, Y. G.; Bartell, L. S. *J. Phys. Chem. B* **1999**, *103*, 11 196. (b) Chushak, Y.; Bartell, L. S. *J. Phys. Chem A* **2000**, *104*, 9328. (c) Huang, J.; Bartell, L. S. *J. Phys. Chem. A* **2002**, *106*, 2404.
(40) Cahn, J. W. *J. Chem. Phys.* **1977**, *66*, 3667.

(41) Djikaev, Y. S.; Tabazadeh, R.; Hamill, P.; Reiss, H. *J. Phys. Chem. A* **2002**, *106*, 10247.
(42) Elbaum, M.; Lipson, S. G.; Das, J. G. *J. Crystal. Growth* **1993**, *129*, 491−505.
(43) Turnbull, D.; Fisher, J. C. *J. Chem. Phys.* **1949**, *17*, 71−73.
(44) Adamson, A. W. *Physical Chemistry of Surfaces*, 5th ed; John Wiley and Sons Inc.: New York, 1990.
(45) Tisdale, R. T.; Middlebrook, A. W.; Prenni, A. J.; Tolbert, M. A. *J. Phys. Chem.* **1997**, *101*, 2112−2119.
(46) Donaldson, D. J.; Anderson, D. *Geophys. Res. Lett.* **1999**, *26*, 3625−3628.
(47) Yang, H.; Finlayson-Pitts, B. J. *J. Phys. Chem.* **2001**, *105*, 1890−1896.
(48) Lin, J. S.; Tabazadeh, A. *J. Geophys. Res.* **2001**, *106*, 4815−4829.